MOLECULAR AND CELLULAR BIOLOGY, Sept. 2009, p. 4935–4948 Vol. 29, No. 18
0270-7306/09/$08.00+0 doi:10.1128/MCB.01705-08

ErbB4 Splice Variants Cyt1 and Cyt2 Differ by 16 Amino Acids and Exert Opposing Effects on the Mammary Epithelium In Vivo▽

Rebecca S. Muraoka-Cook,[1,2] Melissa A. Sandahl,[1] Karen E. Strunk,[1] Leah C. Miraglia,[1] Carty Husted,[1] Debra M. Hunter,[1] Klaus Elenius,[5] Lewis A. Chodosh,[6] and H. Shelton Earp III[1,3,4]*

UNC Lineberger Comprehensive Cancer Center[1] and Departments of Genetics,[2] Medicine,[3] and Pharmacology,[4] University of North Carolina School of Medicine, Chapel Hill, North Carolina 27599; MediCity Research Laboratory, Departments of Medical Biochemistry and Molecular Biology and Department of Oncology, University of Turku, Turku FIN-20520, Finland[5]; and Department of Cancer Biology, Abramson Family Cancer Research Institute, University of Pennsylvania School of Medicine, Philadelphia, Pennsylvania 19104-6160[6]

Received 5 November 2008/Returned for modification 11 December 2008/Accepted 3 July 2009

Data concerning the prognostic value of ErbB4 in breast cancer and effects on cell growth have varied in published reports, perhaps due to the unknown signaling consequences of expression of the intracellular proteolytic ErbB4 $s80^{HER4}$ fragment or due to differing signaling capabilities of alternatively spliced ErbB4 isoforms. One isoform (Cyt1) contains a 16-residue intracellular sequence that is absent from the other (Cyt2). We expressed $s80^{Cyt1}$ and $s80^{Cyt2}$ in HC11 mammary epithelial cells, finding diametrically opposed effects on the growth and organization of colonies in three-dimensional matrices. Whereas expression of $s80^{Cyt1}$ decreased growth and increased the rate of three-dimensional lumen formation, that of $s80^{Cyt2}$ increased proliferation without promoting lumen formation. These results were recapitulated in vivo, using doxycycline-inducible, mouse breast-transgenic expression of $s80^{Cyt1}$ amd $s80^{Cyt2}$. Expression of $s80^{Cyt1}$ decreased growth of the mammary ductal epithelium, caused precocious STAT5a activation and lactogenic differentiation, and increased cell surface E-cadherin levels. Remarkably, ductal growth inhibition by $s80^{Cyt1}$ occurred simultaneously with lobuloalveolar growth that was unimpeded by $s80^{Cyt1}$, suggesting that the response to ErbB4 may be influenced by the epithelial subtype. In contrast, expression of $s80^{Cyt2}$ caused epithelial hyperplasia, increased Wnt and nuclear β-catenin expression, and elevated expression of c-myc and cyclin D1 in the mammary epithelium. These results demonstrate that the Cyt1 and Cyt2 ErbB4 isoforms, differing by only 16 amino acids, exhibit markedly opposing effects on mammary epithelium growth and differentiation.

Activation of the ErbB/HER/epidermal growth factor receptor (ErbB/HER/EGFR) family of receptor tyrosine kinases (RTKs) is often equated with proliferation and oncogenesis. The family consists of four members, HER1/ErbB1/EGFR, HER2/ErbB2/Neu, HER3/ErbB3, and HER4/ErbB4. Each protein has a large NH_2-terminal extracellular domain, a transmembrane domain, and a large intracellular domain with a tyrosine-rich carboxy-terminal region and a tyrosine kinase-like sequence (12). HER1/ErbB1, HER2/ErbB2, and HER4/ErbB4 exhibit ligand-inducible tyrosine kinase activity, whereas HER3/ErbB3 does not.

ErbB receptor activation at the cell surface targets multiple cytoplasmic signaling cascades that transmit signals to the nucleus. In addition to this classic RTK signaling model, ErbB RTKs have exhibited nuclear localization (4, 17, 19, 27, 28, 37, 47, 48). While ErbB1, -2, and -3 are transported to the nucleus as full-length receptors, one isoform of ErbB4 is cleaved upon ligand binding, liberating the entire soluble intracellular domain. This intracellular, kinase-active 80-kDa cleavage product ($s80^{HER4}$) exhibits nuclear-cytoplasmic shuttling (8, 20, 25, 27). Expression of $s80^{HER4}$ mimics certain biological consequences of ligand-induced ErbB4 expression. For example, expression of ligand-induced ErbB4 activates the transcription factor STAT5a in vivo and in cultured human breast cancer cells, as does expression of $s80^{HER4}$ (14, 21, 44). Inhibition of ErbB4 cleavage or its nuclear localization impairs ErbB4-mediated STAT5a activation (25, 46, 48).

Evidence suggests that, whereas ErbB1, -2, and -3 all contribute to proliferation and/or survival of the mammary epithelium, ErbB4 induces specification of the mammary anlagen through induction of LEF1 expression and is required for the lactational differentiation of the mouse mammary gland through activation of STAT5a (13, 38). ErbB4 expression and activity (measured by tyrosine phosphorylation) are lowest during phases of epithelial cell proliferation (puberty and early pregnancy) and highest during phases of differentiation (late pregnancy and early lactation) (35). Mammary glands from mice that lack ErbB4 activity have lactational defects due an impaired program of differentiation (13, 21, 44). Similarly, impaired ErbB4 association with one of its ligands, HB-EGF, causes lactational deficiency (53).

Studies suggests that human ErbB4/HER4 activity decreases growth of several human breast cancer cells (7, 25, 27, 33). However, other evidence shows that ErbB4 expression increases the growth of some estrogen receptor-positive (ER^+) breast cancer cells in culture (15, 22, 55). In similarity to these cell culture studies, there are conflicting reports regarding the prognostic value of ErbB4 expression in human breast cancers.

* Corresponding author. Mailing address: UNC Lineberger Comprehensive Cancer Center, University of North Carolina at Chapel Hill, 102 Mason Farm Road, Chapel Hill, NC 27599. Phone: (919) 966-2335. Fax: (919) 966-3015. E-mail: hse@med.unc.edu.

▽ Published ahead of print on 13 July 2009.

Many reports show that ErbB4 expression correlates with positive prognostic indicators (ER expression, lower tumor grade, increased differentiation, lower proliferative index) and greater disease-free and overall survival (3, 43, 45, 49, 50). However, other reports have presented descriptions of decreased survival in subsets of women whose breast cancers express nuclear ErbB4 (1, 22).

The discrepancy may stem from the different biological properties of the ErbB4 splice variants, of which there are four (5, 6, 16). The JMa isoform harbors a TACE cleavage site in the extracellular domain that is required for the ligand-dependent proteolysis of ErbB4 and subsequent production of $s80^{HER4}$ by γ-secretase (18, 27, 32); the JMb isoform lacks this TACE cleavage site and therefore does not produce $s80^{HER4}$ (6). Splice variations within the cytoplasmic domain generate the Cyt1 and Cyt2 isoforms. Cyt1 contains a 16-amino-acid sequence that is absent from Cyt2 (5). This Cyt1 motif harbors potential binding sites for p85 and WW domain-containing proteins. Signaling differences between ErbB4-Cyt1 and ErbB4-Cyt2 have been previously reported: for example, levels of kinase activity, protein stability, and nuclear accumulation are greater for $s80^{Cyt2}$ than for $s80^{Cyt1}$ (41, 42).

We have directly compared growth and differentiation of mammary epithelial cells expressing $s80^{Cyt1}$ and $s80^{Cyt2}$ in cell culture and in vivo. HC11 cells proliferated rapidly in response to expression of $s80^{Cyt2}$ but exhibited growth inhibition in response to $s80^{Cyt1}$ expression. In three-dimensional (3D) culture experiments, $s80^{Cyt1}$ expression enhanced lumen formation whereas $s80^{Cyt2}$ expression resulted in the growth of large, solid colonies. In the mouse mammary gland, inducible expression of $s80^{Cyt1}$ during puberty decreased proliferation and caused precocious lactogenesis in the ductal epithelium of virgin mice. In contrast, $s80^{Cyt2}$ expression resulted in epithelial hyperplasia.

MATERIALS AND METHODS

Cell culture and transfection. HC11-pcDNA4, HC11-$s80^{Cyt1}$, HC11-$s80^{Cyt2}$, HC11-$s80^{KD}$, HC11-HER4, and HC11-$HER4^{KD}$ cells were previously described (39). pcDNA3-HER4-P1054A cells were made in the laboratory of K. Elenius by side-directed mutagenesis. For 3D cultures, eight-well chamber slides were coated with growth factor-reduced Matrigel (40 μl/well). A total of 5,000 cells/well were plated in 500 μl of serum-free Dubecco's modified Eagle medium/F12-4% growth factor-reduced Matrigel, cultured 14 days, and then fixed in 1% paraformaldehyde–phosphate-buffered saline (1% paraformaldehyde–PBS) and stained with DAPI (4′,6′-diamidino-2-phenylindole) (Vector Laboratories, Burlingame, VT). Colonies were visualized using a Leica SP2 laser scanning confocal microscope with a 63× oil numerical aperture 1.40 Plan Apo lens (Nikon). For growth analysis, cells (0.3×10^6) were plated in 15-cm-diameter dishes at $t = 0$. Media was replaced with serum-free media at $t = 4$ h. Three plates per cell type per set of conditions were collected by trypsinization at 24-h intervals and manually counted daily for 96 h. For immunocytofluorescence, cells were cultured on glass slides, fixed in ice-cold methanol for 10 min, washed in PBS, and then incubated in mouse monoclonal β-catenin antibody (Sigma-Aldrich, St. Louis, MO) diluted 1:500 in PBS. After five consecutive washes in PBS, slides were incubated in Alexa Fluor 488-conjugated goat anti-mouse immunoglobulin G (Molecular Probes, Invitrogen, Carlsbad, CA), washed, and mounted with Vectashield (Vector Labs, Burlingame, VT).

Cell and tissue preparation and Western analysis. NE-PER nuclear and cytoplasmic extraction reagents (Pierce Biotechnology, Rockford, IL) were used to separate nuclear and cytoplasmic compartments of cells in accordance with the manufacturer's protocol. ErbB4 and green fluorescent protein (GFP) immunoprecipitations (IPs) were performed using rabbit polyclonal antibody 132 and anti-GFP (Santa Cruz Biotechnologies, Santa Cruz, CA) as previously described (33). Western analyses were performed as previously described (25) using PY20 antibody (Santa Cruz) directed against phosphotyrosine or anti-ErbB4 132 antibody produced in our laboratory (25).

Flow cytometric analysis. Cells were collected by trypsinization and fixed in 1% paraformaldehyde. Cells were stained for terminal deoxynucleotidyltransferase-mediated dUTP-biotin nick end labeling (TUNEL) analysis using an Apobromodeoxyuridine (Apo-BrdU) staining kit (Chemicon, Temecula, CA) according to the manufacturer's directions. For cell cycle analyses, cells were stained with propidium iodide-RNase solution (Sigma-Aldrich) according to the manufacturer's directions. Cells were analyzed using a FACScan system at the University of North Carolina (UNC) Lineberger Comprehensive Cancer Center Flow Cytometry Core Facility at the UNC at Chapel Hill.

Generation and analysis of TetOp-$s80^{Cyt1}$ and TetOp-$s80^{Cyt2}$ mice. A 2.2-kb cDNA fragment, encoding the entire intracellular domain of human ErbB4-Cyt1 and ErbB4-Cyt2 and tagged at the amino terminus with GFP, was subcloned into pTRE-Tight (BD Biosciences) at the BamHI-NotI sites. The linearized transgene was injected into one-cell-stage FVB mouse embryos and transplanted into pseudopregnant females (Mouse Models Core Facility, UNC Lineberger Comprehensive Cancer Center). The resulting pups were screened for genomic transgene insertion using primers P1 (from a human ErbB4 sequence; 5′-TCC TCT AGA GAT ATC GTC GAC AAG CTT ATC-3′) and P2 (from pTRE-Tight; 5′-CGG AGC ACC CTT CAG CAC CCA GAC-3′). All transgenic founders were bred to inbred FVB mice harboring the mouse mammary tumor virus-reverse tetracycline transcriptional activator (rtTA) transgene (MTB mice) (10). All founders transmitted the transgene to their offspring. Each resulting transgenic line was independently analyzed. All studies were performed using age-matched females of the F1 or F2 generation. For timed pregnancies, mating pairs were established and mice were monitored daily for vaginal plugs, indicating 0.5 days postcoitum (dpc). The day of partuition was designated lactation day 1 (L1).

Histological analysis and IHC. Mice were labeled for 2 h with BrdU (Sigma-Aldrich) (10 mg/kg of body weight) by intraperitoneal injection. Mammary glands were fixed in 10% formalin (VWR Scientific). Hematoxylin-stained whole mounts of no. 4 (right inguinal) mammary glands were prepared as previously described (23). Paraffin-embedded mammary glands were sectioned (in 5-μm-thick sections) and rehydrated, and immunohistochemistry (IHC) was performed as previously described (23) using the following antibodies: GFP (1:100), from Santa Cruz Biotechnologies, Santa Cruz, CA; phospho-Ser10 histone H3 (p-HH3) (1:200) and cyclin D1 (1:100), both from Cell Signaling; STAT5a (1:100) and phosphotyrosine 694 STAT5A/STAT5B (1:50), BrdU (1:500), and E-cadherin (1:100), all from Invitrogen-Zymed; and c-myc (1:500) and β-catenin (1:1,000), from Sigma-Aldrich. Slides were washed in PBS (pH 7.4)–0.1% Tween 20, and then staining was visualized with a Vectastain kit (Vector Laboratories, Burlingame, VT). Cells were photographed using a Nikon FXA microscope and Scion Image 2.0 software.

Northern analysis and RT-PCR. Total RNA was extracted using TRIzol reagent (Invitrogen) according to the manufacturer's directions. Total RNA (10 μg) was resolved on a 1.0% agarose-formaldehyde gel and transferred to nitrocellulose with 10× sodium saline citrate (Invitrogen). Membranes were hybridized with a mouse β-casein cDNA probe (EcoRI fragment of EST clone 5026838; Invitrogen, Carlsbad, CA) that was labeled with biotin by the use of a North2South random primer labeling kit (Pierce Biotechnology, Rockford, IL). Membranes were hybridized, washed, and developed using a North2South nonradioactive hybridization kit (Pierce Biotechnology). Reverse transcriptase PCR (RT-PCR) was performed as described previously (25). Primers for identification of mouse Wnt1, mouse Wnt2, mouse Wnt5b, mouse Wnt7a, mouse Wnt10b, mouse LEF1, and mouse GATA3 are listed in Table 1.

RESULTS

Growth inhibition of HC11 cells by expression of $s80^{Cyt1}$ but not that of $s80^{Cyt2}$. We expressed GFP-tagged constructs of $s80^{Cyt1}$ and $s80^{Cyt2}$ in the mouse mammary epithelial cell (MEC)-derived HC11 cell line. Pooled clones of stably transfected cells were used to compare the growth rates of HC11-pcDNA4, HC11-$s80^{Cyt1}$, HC11-$s80^{Cyt2}$, and HC11-$s80^{KD}$ cells (expressing kinase-dead $s80^{Cyt1}$). HC11-pcDNA4 cells grew steadily over 96 h, resulting in a 6.0-fold increase in total cell numbers (Fig. 1A). HC11-$s80^{Cyt1}$ cells grew more slowly than HC11-pcDNA4 cells (4.2-fold increase in total cell numbers over 96 h; $P = 0.011$), whereas HC11-$s80^{Cyt2}$ cells grew more rapidly (9.2-fold increase at 96 h; $P = 0.007$). Expression of

TABLE 1. Primer sequences used for the detection of the indicated transcripts by RT-PCR[a]

cDNA	Position (residues)	Forward primer	Reverse primer
Wnt1	1141–1381	AGC TGC TGC GCC TGG AGC CC	GCT GAC GTG GCA AGC ACC AG
Wnt2	721–1001	AGG ACA TGC TGG CTG GCC AT	TCA TAG CCT CTC CCA CAA CA
Wnt5b	1021–1171	ACA GAA CAA CGA GGC TGG CC	GGC GCT GTC GTA CTT CTC CT
Wnt7	1021–1261	TCA AGA AGC CCC TGT CCT AC	GCT GCA CGT GTT ACA CTT GA
Wnt10b	1201–1471	CAA CTC TGG AGC GTT CCA GC	CTC TGT GAC TTT ACA CTC AT
LEF1	1561–1771	CAG CTC CTG AAA TCC CCA CC	GCT GGA TGA GGG ATG CCA GT
Gata3	1441–1681	TGC AAT GCC TGC GGA CTC TA	CTA GAC ATC TTC CGG TTT CG

[a] Primer sequences were designed from NCBI-published cDNA sequences derived from mouse genes. The residue numbers corresponding to each primer set are shown and were used to predict the size of each amplicon. Primer sequences are shown in 5′-to-3′ orientation.

GFP-s80^{Cyt1} and GFP-s80^{Cyt2} was observed at higher levels than that seen with endogenous full-length ErbB4/HER4 and s80, its endogenous proteolytic product, in HC11 cells. Western analysis of HER4 IPs from cytoplasmic and nuclear extracts demonstrated that GFP-s80^{Cyt2} and GFP-s80^{Cyt1} localized to nuclear and cytoplasmic compartments whereas GFP-s80^{KD} was restricted to the cytoplasm (Fig. 1C). The requirement of kinase activity for nuclear accumulation of s80^{HER4} has been previously demonstrated (8, 25, 39). We have shown that expression of GFP-s80^{Cyt1} in HC11 cells results in decreased growth due to a decreased rate of cellular proliferation (8). The intracellular domain of ErbB4 has been reported to increase apoptosis of mammary epithelial cells (26). To determine the effects of s80^{Cyt1} and s80^{Cyt2} overexpression on apoptosis in HC11 cells, we used TUNEL analysis to detect and enumerate apoptotic cells (Fig. 1D). Expression of GFP-s80^{Cyt1} resulted in a higher (threefold) increase in the proportion of cells undergoing apoptosis ($P < 0.02$). These data suggest that increased cell death, combined with decreased cellular proliferation in response to s80^{Cyt1} expression, accounts for the decrease in HC11 cell numbers in culture under these growth conditions.

HC11 cells grow as acinar structures in three dimensions in response to the presence of prolactin, in response to ligand-inducible ErbB4-JMa-Cyt1 activity, and in response to the presence of exogenous GFP-s80^{Cyt1} (25, 52). The latter deter-

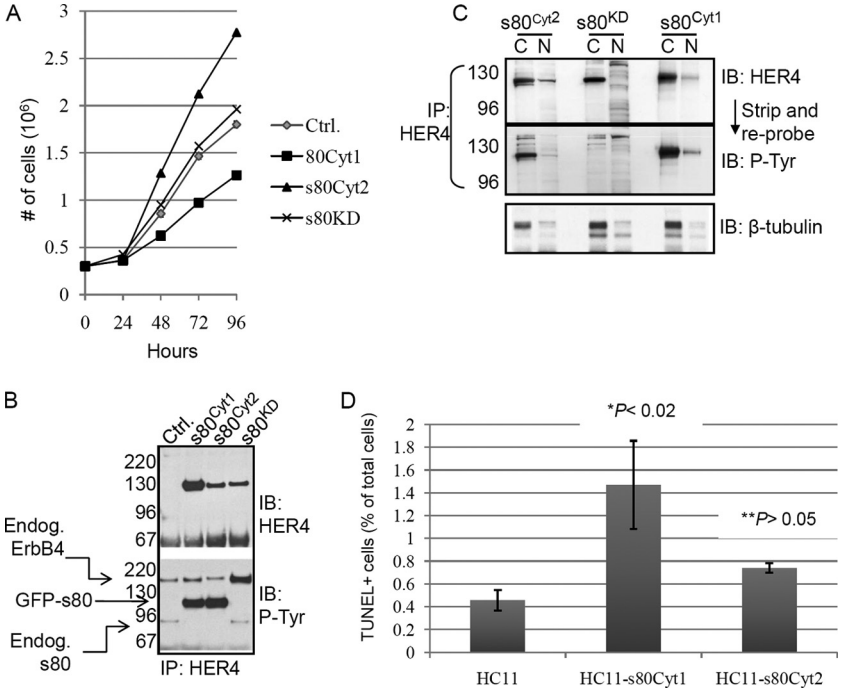

FIG. 1. Growth inhibition induced by s80^{Cyt1} and growth acceleration induced by s80^{Cyt2}. (A) Growth analysis of HC11-pcDNA4, HC11-s80^{Cyt1}, HC11-s80^{Cyt2}, and HC11-s80^{KD} cells. Values represent average numbers of cells. Data represent values ± standard deviations determined in three experiments, each analyzed in duplicate. (B) HER4 IPs were subjected to Western analysis to detect total levels of HER4 and phosphotyrosine (P-Tyr). Molecular weights are indicated to the left of each panel. IB, immunoblot. (C) HER4 IP from nuclear (represented by the letter N) and cytoplasmic (represented by the letter C) extracts of HC11-s80^{Cyt1}, HC11-s80^{Cyt2}, and HC11-s80^{KD} cells. IPs were subjected to Western blot analysis with phosphotyrosine or ErbB4 antibodies. Nuclear and cytoplasmic extracts were subjected to Western analysis to detect β-tubulin to verify the relative purity of the cellular fractionation. (D) TUNEL analysis of cells by the use of a phycoerythrin-conjugated anti-BrdU antibody to detect BrdU-labeled apoptotic cells. Flow cytometry was used to detect TUNEL-positive DAPI-stained cells. Quantitation of the proportion of TUNEL-positive cells is shown. Values represent the averages of the results of three experiments, each analyzed in duplicate. Error bars represent standard deviations.

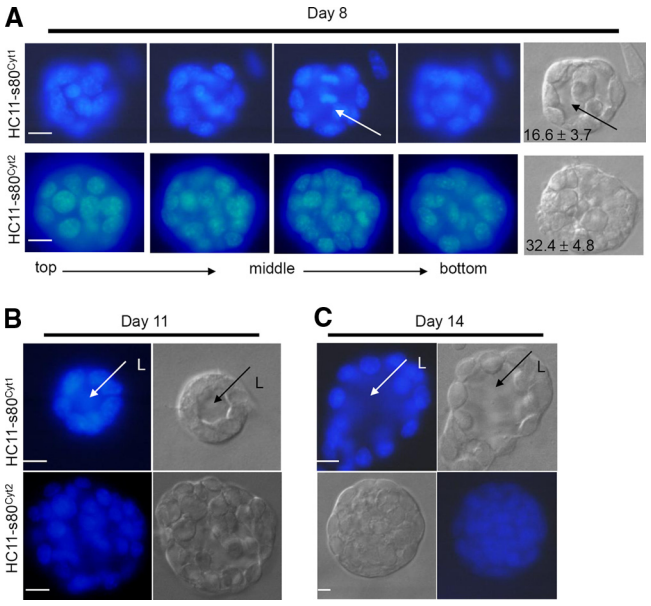

FIG. 2. Lumen formation in cells expressing $s80^{Cyt1}$ but not $s80^{Cyt2}$. Cells were cultured in 3D-Matrigel and stained using DAPI and photographed on days 8 (A), 11 (B), and 14 (C). Arrows in panels indicate lumen (L) formation. (A) Confocal microscopy-acquired serial Z-plane sections through DAPI-stained colonies. A single differential interference-contrast image is shown to the right of each series. Numbers in the right panels represent average numbers of cells/colony (n = 30; P = 0.002 [Student's unpaired t test]). (B and C) Single-plane sections are shown for each colony at day 11 (B) and day 14 (C). DAPI-staining images are at the left side of the figure; DIC images are at the right. Scale bars, 50 μm. Note that a lower magnification was used for the $s80^{Cyt2}$ image in panel C in order to visualize the entire HC11-$s80^{Cyt2}$ colony.

mination was confirmed, as shown by examination of serial Z-plane sections of HC11-$s80^{Cyt1}$ colonies (Fig. 2A). In contrast, HC11-$s80^{Cyt2}$ colonies formed solid structures filled with cells. By day 11 and through day 14, HC11-$s80^{Cyt1}$ colonies harbored distinct lumens surrounded by a single cell layer (Fig. 2B and C). HC11-$s80^{Cyt2}$ colonies did not display lumen formation at day 11 or 14 but displayed increased colony size and numbers of cells per colony (1.95-fold more cells/colony in HC11$s80^{Cyt2}$ compared to HC11-$s80^{Cyt1}$; n = 30). Therefore, expression of $s80^{Cyt1}$ and $s80^{Cyt2}$ impacts the structural differentiation of HC11 cells with opposing outcomes.

The WW-domain binding motif is required for HER4-mediated growth inhibition. Cyt1 contains a 16-amino-acid sequence absent from Cyt2 (5). This Cyt1 motif harbors potential binding sites for p85 (amino acids 1056 to 1059, YXXM) and WW domain-containing proteins (amino acids 1052 to 1056, PPPAY). Our previous results demonstrated that overexpression of HER4-JMa-Cyt1 in HC11 cells decreased growth while enhancing differentiation (25) and that WW-domain-containing proteins bind to the HER4 cytoplasmic domain to regulate HER4 signaling. To determine whether the WW-domain binding motif of HER4-JMa-Cyt1 was important for HER4-mediated growth inhibition, a single proline 1054-to-alanine point mutation (termed $HER4^{P1054A}$) within HER4-JMa-Cyt1 was engineered in the laboratory of K. Elenius. This mutation disrupts the consensus WW-domain binding motif (41, 42). HER4-JMa-Cyt1 (referred to here as HER4), $HER4^{P1054A}$, and kinase-dead HER4-JMa-Cyt1 (referred to here as $HER4^{KD}$) were expressed by stable transfection in HC11 cells. HER4 and $HER4^{P1054A}$ were detected at 185 kDa and 80 kDa, suggesting that both of these HER4-JMa variants are able to undergo γ-secretase-mediated cleavage to generate $s80^{HER4}$ (Fig. 3A). $HER4^{KD}$ was not detected at 80 kDa, which is consistent with previous observations that HER4-JMa requires kinase activation and tyrosine phosphorylation prior to proteolytic cleavage (39).

Growth of HC11 cells was determined after 96 h of culture in the presence or absence of heregulin β1 (HRG), the HER4 ligand. Treatment of parental HC11 cells, but not HC11-HER4 cells, with HRG resulted in a 1.9-fold increase in cell numbers compared to untreated parental HC11 cell results, which is consistent with previous determinations that increased HER4-JMa-Cyt1 expression confers growth inhibition to HC11 cells (Fig. 3B). In contrast, expression of HER4-P1054A increased growth of HC11 cells under basal conditions and in response to the presence of HRG, suggesting that this WW-domain interaction motif may be involved in HER4-directed growth inhibition.

In previous studies using human breast cancer cells, HER4 activation was shown to delay G_2/M progression in cycling cells. Whereas ErbB4/HER4 is endogenously expressed in HC11 cells, we found that HRG-treated HC11 cells did not accumulate in the G_2/M phase in response to the treatment with HRG (Fig. 3C). However, overexpression of HER4-JMa-Cyt1 resulted in a small but significant increase in the G_2/M population under basal conditions, and the rate of increase was further enhanced in response to treatment with HRG (Fig. 3D). G_2/M accumulation was not observed in HC11 cells expressing HER4-P1054A or in cells expressing $HER4^{KD}$. These data suggest that the WW-domain binding motif may be required for HER4-meditated growth inhibition in HC11 cells, in part through decreasing the rate of transit through the G_2/M phase.

Nuclear and cytoplasmic expression of $s80^{Cyt1}$ and $s80^{Cyt2}$ in the mammary epithelium in vivo. To assess the effects of $s80^{Cyt1}$ and $s80^{Cyt2}$ expression on growth and differentiation of MECs in vivo, TetOp-$s80^{Cyt1}$ and TetOp-$s80^{Cyt2}$ transgenes were constructed that contained a doxycycline (DOX)-inducible rtTA-dependent promoter driving expression of either GFP-$s80^{Cyt1}$ or GFP-$s80^{Cyt2}$. The transgenes were injected into one-cell-stage mouse embryos, generating four independent transgenic founders for TetOp-$s80^{Cyt1}$ and three independent founders for TetOp-$s80^{Cyt2}$ (referred to hereafter as TetOp-Cyt1 and TetOp-Cyt2). Each transgenic founder was crossed with mice harboring the mouse mammary tumor virus-rtTA transgene (MTB mice) (10). DOX-inducible transgenic expression of the GFP-tagged $s80^{Cyt1}$ and $s80^{Cyt2}$ products was examined in 4-week-old double transgenic F1 offspring treated for 48 h with DOX. Western analysis to detect HER4 in GFP IPs from whole mammary extracts demonstrated DOX-inducible expression of GFP-$s80^{Cyt1}$ in MTB/Cyt1 mice but not in TetOp-Cyt1 mice (Fig. 4A). Similarly, GFP-$s80^{Cyt2}$ was detected in DOX-treated MTB/Cyt2 but not TetOp-Cyt2 mice. IHC detection of GFP specifically in the mammary epithelium was detected in MTB/Cyt1 and MTB/Cyt2 mice treated with DOX but not in vehicle-treated mice (Fig. 4B).

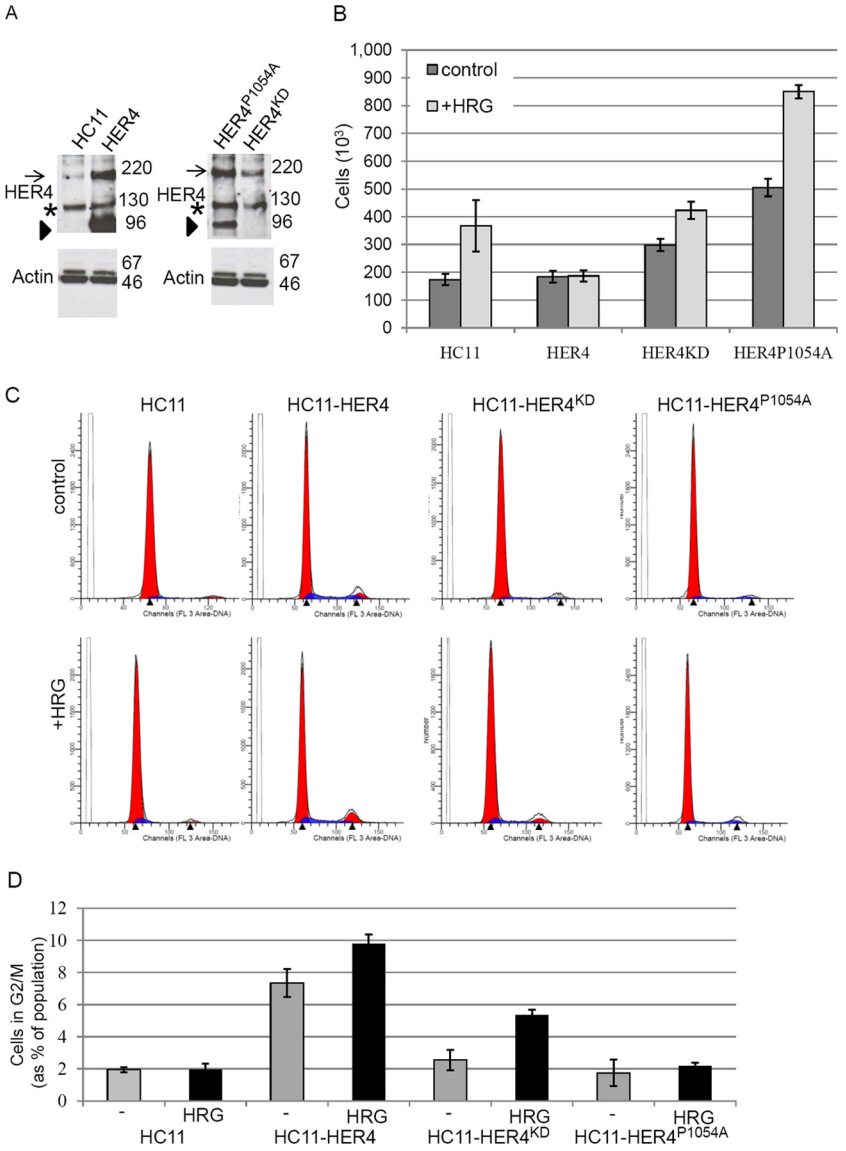

FIG. 3. The WW-domain binding motif within HER4-Cyt1 is important for HER4-mediated growth inhibition. (A) Expression of human HER4-JMa-Cyt1, and of the P1054A point mutation that abrogates WW domain binding, in HC11 cells cultured in serum-free media and stimulated for 30 min with HRG (10 ng/ml). Kinase-dead HER4^{KD} harbors a Lys-to-Ala mutation within the ATP binding pocket of the kinase domain (see Fig. 1 and references 24 and 25). Western analysis of HER4 IPs and whole-cell lysates detected total HER4 and alpha-actin, respectively. The positions of full-length HER4 (arrows) and the s80/m80 cleavage product of HER4 (arrowheads) are indicated. Nonspecific bands are indicated (*). Molecular weights are indicated at the right side of each panel. (B) Growth analysis of HC11, HC11-HER4, HC11-HER4^{KD}, and HC11-HER4^{P1054A} cells cultured in the presence or absence of HRG (2 ng/ml) for 96 h. A total of 10^5 cells were plated and were counted 96 h after plating. Values represent average numbers of cells ± standard deviations determined in three experiments, each analyzed in duplicate. (C) Cells were plated in media containing 10% serum and harvested 24 h after plating. Cells were stained with propidium iodide and analyzed by flow cytometry to determine DNA content per cell. (D) Quantitation of the number of cells containing 4 N DNA. Values represent the averages of the results of three experiments; each sample was analyzed in triplicate. Error bars indicate standard deviations.

The majority of the GFP$^+$ MECs expressing GFP-s80^{Cyt1} and GFP-s80^{Cyt2} displayed both nuclear and cytoplasmic localization of the GFP-tagged product (Fig. 4C). However, a significantly greater amount of cells with strictly nuclear localization was observed with GFP-s80^{Cyt2} compared to GFP-s80^{Cyt1}, which is consistent with previous reports demonstrating increased nuclear localization and/or accumulation of s80^{Cyt2} (42).

Histologic examination of hematoxylin- and eosin-stained mammary sections from virgin females at 6 months of age revealed significant differences between mammary glands expressing GFP-s80^{Cyt1} and GFP-s80^{Cyt2} and vehicle-treated controls (Fig. 4D, E, and G, showing additional images taken from individual DOX-treated samples). In contrast to the narrow lumens in mammary glands of vehicle-treated mice, the ducts of DOX-treated MTB/Cyt1 mice were distended with secretory material that included fat globules, suggesting an enhanced degree of lactogenic differentiation driven by GFP-

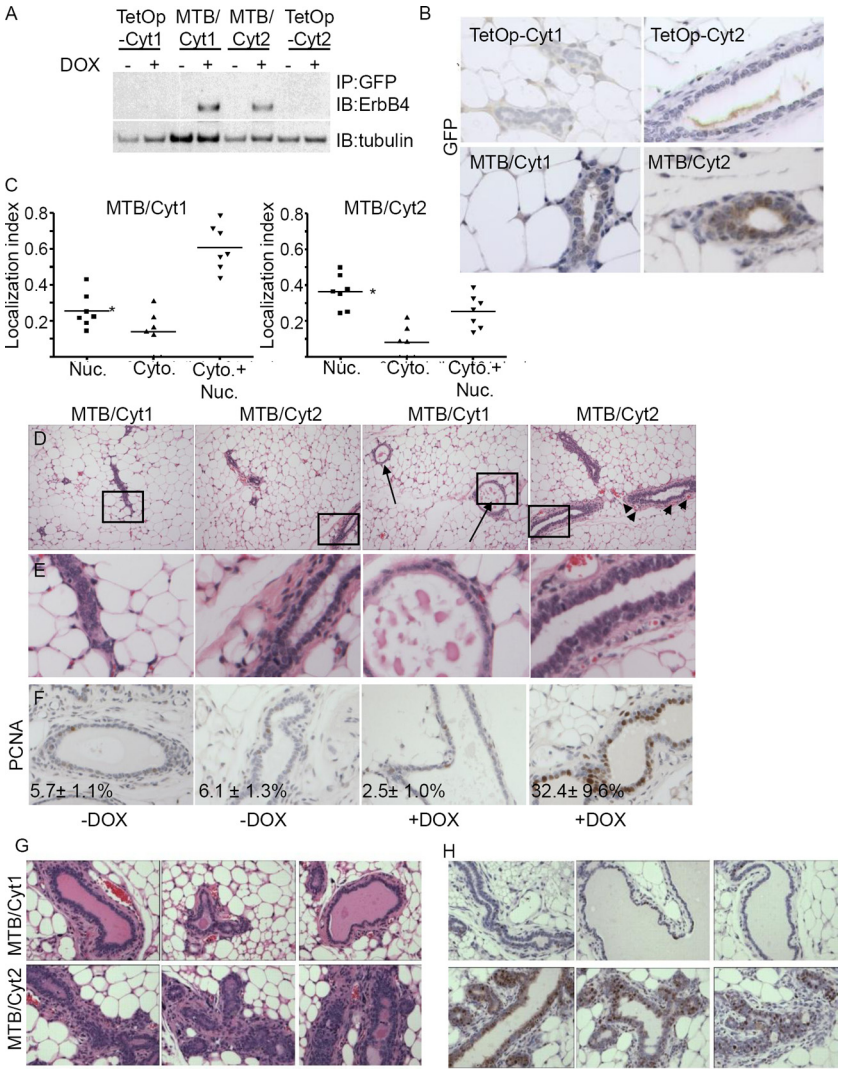

FIG. 4. Expression of s80^{Cyt1} decreases mammary ductal growth, but expression of s80^{Cyt2} increases ductal growth. (A and B) Mice (4 weeks old) were treated with DOX for 48 h or left untreated. (A) Transgene expression was analyzed by IP of GFP followed by immunoblotting (IB) for ErbB4. Whole mammary lysates were analyzed by IB for beta-tubulin. (B) IHC to detect GFP. Representative photomicrographs are shown. (C) All GFP$^+$ cells (10 fields/sample) were scored for GFP in the nucleus (Nuc.) or in the cytoplasm (Cyto.) or in both the nucleus and cytoplasm. Individual data points indicate the following: [number of GFP$^+$ cells in specific compartment ÷ total number of GFP$^+$ cells]. The midlines indicate the average value for each group. * indicates $P < 0.001$ (Student's unpaired t test; $n = 7$). (D and E) Hematoxylin- and eosin-stained mammary glands of 6-month-old mice treated with DOX since 3 weeks of age or left untreated. The boxed areas in panel D are shown at higher magnification in panel E. Arrows indicate filled lumens in DOX-treated MTB/Cyt1 mice. Arrowheads indicate numerous periductal blood vessels in DOX-treated MTB/Cyt2 mice. (F) IHC detection of PCNA in 6-month-old female mice. Values shown at bottom right of each panel indicate the percentage of the total epithelial population that stained positive for PCNA and represent the average results determined with five randomly chosen fields from mammary gland sections derived from five mice per group examined at a magnification of ×400. (G and H) Mammary glands were harvested from virgin female mice 15 weeks of age. (G) Hematoxylin- and eosin-stained mammary gland sections obtained from mice expressing s80^{Cyt1} (top row) or s80^{Cyt2} (bottom row) in the mammary epithelium in response to DOX treatment beginning at 3 weeks of age and persisting until 15 weeks of age. (H) Immunohistochemical detection of PCNA in mammary sections harvested from virgin female mice treated with DOX from 3 weeks of age until 15 weeks of age to induce expression of s80^{Cyt1} (upper panel) or s80^{Cyt2} (bottom panel).

s80^{Cyt1}. In contrast, mammary ducts of DOX-treated MTB/Cyt2 mice were not distended with secretory material and displayed thickened ductal epithelium containing multiple cell layers and numerous mitotic figures. IHC detection of proliferating cell nuclear antigen (PCNA) was increased in the ductal epithelium of DOX-treated MTB/Cyt2 mice compared to vehicle-treated controls (Fig. 4F and H, showing additional representative images taken from individual DOX-treated samples). PCNA was rarely found in the quiescent ductal epithelium of DOX-treated MTB/Cyt1 mice. These results suggest that whereas GFP-s80^{Cyt1} expression confers differentiation to MECs, GFP-s80^{Cyt2} causes hyperplasia.

Pubertal growth of the mammary epithelium is decreased by expression of s80^{Cyt1} but increased by that of s80^{Cyt2}. DOX treatment beginning at 3 weeks of age induced transgene expression at the onset of puberty. Mammary glands were exam-

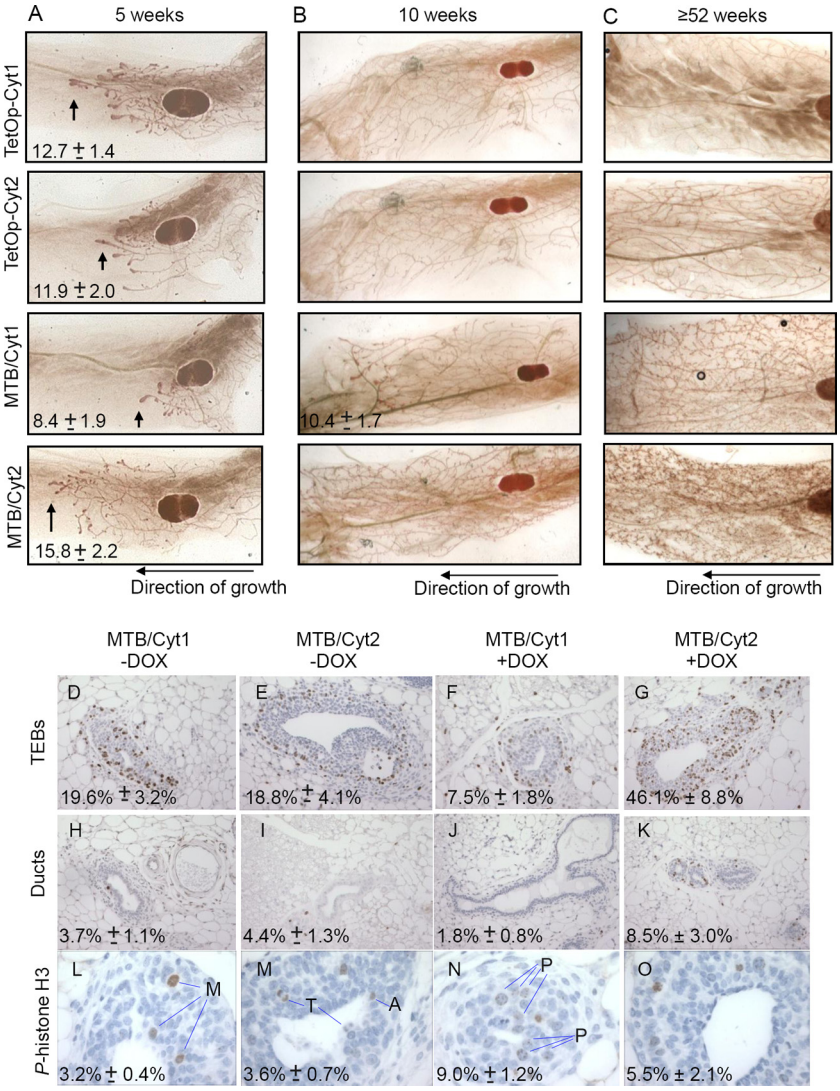

FIG. 5. Epithelial proliferation increased via $s80^{Cyt2}$ expression but decreased via $s80^{Cyt1}$ expression. (A to C) Whole-mount hematoxylin staining of mammary glands from DOX-treated mice at (A) 5 weeks, (B) 10 weeks, and (C) 52 weeks or later. Vertical arrows indicate TEBs at 5 weeks. Data represent average numbers of TEBs ± standard deviations. (D to K) IHC to detect BrdU in TEBs (D to G) and ducts (H to K) from 5-week-old mice. Epithelial cells in five random fields per sample ($n = 4$) were scored as $BrdU^+$ or $BrdU^-$. Data represent percentages of epithelial population that were $BrdU^+$ and are shown as average percentages ± standard deviations. *, $P = 0.033$, Student's unpaired t test. (L to O) Immunostaining for p-HH3 (*P*-histone H3) in TEBs from 5-week-old mice. Arrows indicate positive nuclei. Data indicate percentages of the total epithelial cell population (± standard deviations) that were $p\text{-}HH3^+$. M, metaphase DNA; A, anaphase DNA; T, telophase DNA.

ined at 5 weeks of age (i.e., after 2 weeks of DOX treatment; Fig. 5A). Whole mounted hematoxylin-stained mammary glands of DOX-treated MTB/Cyt1 mice revealed decreased lengthening of the ductal epithelium into the fat pad of the developing breast compared to those of DOX-treated TetOp-$s80^{Cyt1}$ mice. In contrast, the MTB/Cyt2 ductal epithelium advanced further than what was observed in DOX-treated TetOp-Cyt2 mammary glands. Terminal end buds (TEBs), distal club-shaped epithelial structures, represent the most proliferative compartment of the pubertal mammary epithelium. Fewer TEBs were seen in DOX-treated MTB/Cyt1 mammary glands, whereas more TEBs were seen in MTB/Cyt2 mice, compared to single transgenic controls.

At 10 weeks of age, the DOX-treated MTB/Cyt1 epithelium had not fully permeated the fat pad and displayed persistent TEBs, unlike what was seen in DOX-treated MTB/Cyt2, TetOp-Cyt2, and TetOp-Cyt1 mammary glands (Fig. 5B). Decreased ductal elongation in DOX-treated MTB/Cyt1 mice was observed in each of the four TetOp-Cyt1 transgenic mouse lines, whereas an increased rate of ductal extension in DOX-treated MTB/Cyt2 mice was observed with all three TetOp-Cyt2 mouse lines. By 16 weeks of age, the mammary epithelium of DOX-treated MTB/Cyt1 mice fully penetrated the fat pad and TEBs had regressed (data not shown). We restricted the remainder of our analysis of TetOp-Cyt1 mice to mice derived from transgenic line 32 and of TetOp-Cyt2 mice to transgenic line 2.

Mammary glands from aged virgin female mice (52 weeks of

age or older) treated with DOX since 3 weeks of age were examined by whole-mount hematoxylin staining (Fig. 5C). Increased numbers of lobuloalveolar (LA) buds were seen along the ductal epithelium of the mammary glands expressing GFP-s80^{Cyt1} compared to the quiescent ductal epithelium seen in controls. Mammary glands expressing s80^{Cyt2} showed a remarkable increase in epithelial density compared to single transgenic controls, which is consistent with an elevated rate of proliferation in the mammary epithelium due to the expression of GFP-s80^{Cyt2}.

Within TEBs and the ductal epithelium, expression of s80^{Cyt1} decreases cellular proliferation, whereas that of s80^{Cyt2} increases cellular proliferation. We examined the rate of cellular proliferation in DOX- and vehicle-treated MTB/Cyt1 and MTB/Cyt2 mice at 5 weeks of age (i.e., after 2 weeks of DOX treatment) by the use of IHC detection of BrdU incorporation into genomic DNA. TEBs in DOX-treated MTB/Cyt1 mice displayed a 2.6-fold reduction in BrdU incorporation compared to TEBs from vehicle-treated MTB/Cyt1 mice (Fig. 5D to G). In contrast, BrdU incorporation was increased in TEBs from DOX-treated MTB/Cyt2 mice by 2.4-fold over TEBs in vehicle-treated MTB/Cyt2 mice.

Within the ductal epithelium of 5-week-old mice, DOX-treated MTB/Cyt1 mice again demonstrated decreased BrdU incorporation versus vehicle-treated controls (Fig. 5H to K). In contrast, the ductal epithelium of DOX-treated MTB/Cyt2 was highly proliferative, displaying a 2.2-fold increase in BrdU incorporation compared to vehicle-treated controls.

Despite the decreased cellular proliferation in DOX-treated MTB/Cyt1 samples, as measured by PCNA and BrdU levels, an increased rate of formation of early mitotic cells was observed in TEBs from DOX-treated MTB/Cyt1 mice (Fig. 5L to O). Using p-HH3 as a mitotic marker, a threefold increase in mitotic cell levels was seen in TEBs from DOX-treated MTB/Cyt1 mice compared to untreated controls. Examination of p-HH3 subnuclear patterning demonstrated that the majority of p-HH3 appeared in a diffuse and punctate nuclear pattern in DOX-treated MTB/Cyt1 samples, which is consistent with the earliest stages of mitosis (prophase). In contrast, nuclei from untreated controls showed p-HH3 patterns representing each of the stages of mitosis (prophase, metaphase, anaphase, and telophase). This suggests that decreased transit through early mitosis is one reason for the delayed growth rate of MECs expressing GFP-s80^{Cyt1}. These data are consistent with previous reports that expression of ErbB4-Jma-Cyt1 and s80^{Cyt1} decreased the rate of cell cycle progression through the G_2/M phase in many, but not all, breast cancer cell lines (33, 24, 39).

Expression of s80^{Cyt1} but not s80^{Cyt2} induces STAT5a phosphorylation and milk gene expression in mammary glands of virgin mice. Lipid accumulation was consistently seen in mammary glands from virgin DOX-treated MTB/Cyt1 mice but not in virgin DOX-treated MTB/Cyt2 mice (see Fig. 4). Mammary glands from 6-month-old virgin mice (treated with DOX since the age of 3 weeks or left untreated) were assessed for markers of lactogenic differentiation, including STAT5a phosphorylation and nuclear localization, and expression of β-casein, a milk protein. Subcellular localization of STAT5a was examined by IHC (Fig. 6A to D). In samples from DOX-treated MTB/Cyt1 mice, luminal epithelial cells expressed abundant nuclear STAT5a (Fig. 6C). DOX-treated MTB/Cyt2 mammary glands expressed only moderate levels of STAT5a with mixed cytoplasmic and nuclear localization (Fig. 6D), in similarity to vehicle-treated controls (Fig. 6A to B). In 6-month-old mice, expression of β-casein mRNA was detected in RNA samples harvested from mammary glands expressing GFP-s80^{Cyt1} but not in those from mammary glands expressing GFP-s80^{Cyt2} or in those from DOX or vehicle-treated controls (Fig. 6E).

To assess whether short-term GFP-s80^{Cyt1} expression could induce STAT5a activity in virgin mice, MTB/Cyt1 mice were treated with DOX for 96 h. Phosphotyrosine 694 STAT5A/STAT5B and β-casein mRNA expression was abundant in the mammary epithelium of DOX-treated MTB/Cyt1 mice but not in that of vehicle-treated mice (Fig. 6F to H). Taken together, these results suggest that expression of s80^{Cyt1}, but not that of s80^{Cyt2}, is sufficient to rapidly induce some of the molecular aspects of lactogenic differentiation in virgin mice in vivo in the absence of hormonal signals that normally influence lactogenesis.

s80^{Cyt1} does not impair alveolar proliferation during pregnancy. During pregnancy, rapid cellular proliferation and differentiation of the LA epithelium generates the milk-producing structures of the mammary gland. To determine the effects of GFP-s80^{Cyt1} expression on proliferation of the LA and ductal epithelium specifically during pregnancy, DOX was withheld from mice until timed pregnancies were established in 12-week-old virgin mice. DOX treatment began at 0.5 dpc and lasted through L10. Areas of focal hyperplasia were seen in lactating mammary glands from DOX-treated MTB/Cyt2 mice but not in those from DOX-treated MTB/Cyt1 mice (Fig. 6I to L). Despite this, results with respect to differentiation of the mammary epithelium appeared to be similar in all samples. Control, MTB/Cyt1, and MTB/Cyt2 mammary glands displayed increased LA epithelial content composed of lipid-producing secretory cells, milk-filled lumens, and few visible adipocytes. MTB/Cyt1 and MTB/Cyt2 mothers were able to successfully nurse pups through weaning (21 days). Therefore, expression of GFP-s80^{Cyt1} or GFP-s80^{Cyt2} does not adversely affect pregnancy-induced lactogenic differentiation of the mammary gland, which is consistent with the proposed role of ErbB4 in lactogenesis. However, these data also suggest that GFP-s80^{Cyt1} expression did not impair pregnancy-induced proliferation of the LA epithelium, in contrast to the ductal epithelial cell growth inhibition observed during puberty.

To examine proliferation within specific epithelial compartments (ductal versus LA) during pregnancy, PCNA expression was examined by IHC. No statistically significant differences in PCNA staining of the LA epithelium between samples from vehicle-treated mice and those from DOX-treated MTB/Cyt1 mice or MTB/Cyt2 mice were observed (Fig. 7A to C and G). However, the ductal epithelium of DOX-treated MTB/Cyt1 mice displayed fewer PCNA$^+$ cells (19 out of 322 ductal cells) compared to the ducts of vehicle-treated MTB/Cyt1 mice (56 out of 310 cells; $P < 0.001$). In contrast, the ductal epithelium of DOX-treated MTB-Cyt2 mammary glands displayed a dramatic increase in the PCNA-positive population (172/333; $P < 0.001$), again emphasizing the opposing effects of the presence of Cyt2 and Cyt1 HER4 isoforms.

At L10, PCNA$^+$ cells in the LA epithelium in mammary glands from DOX-treated and vehicle-treated MTB/Cyt1 mice were similar, again suggesting that expression of s80^{Cyt1} does

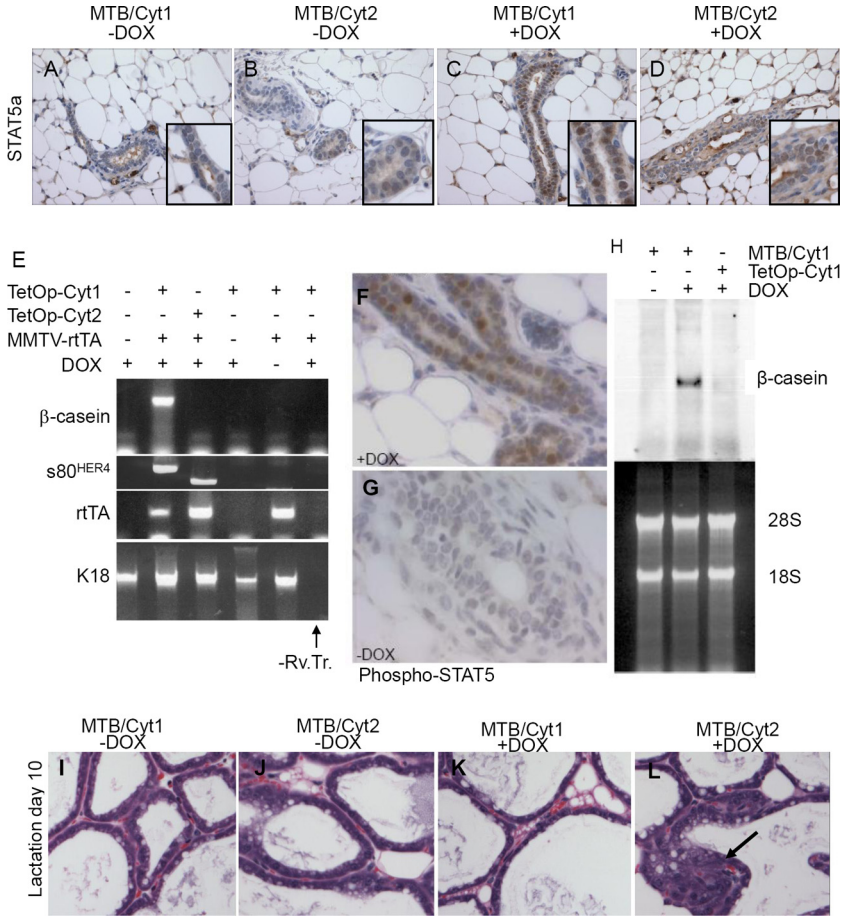

FIG. 6. Precocious differentiation and STAT5a activation in mammary glands expressing $s80^{Cyt1}$ but not $s80^{Cyt2}$. (A to D) STAT5a IHC analysis using mammary glands from 6-month-old virgin female mice. Representative photomicrographs are shown ($n = 5$ per group). Insets show views at higher magnification. (E) RT-PCR of total mammary RNA harvested from mice 6 months of age. RNA samples from three mice per genotype were pooled prior to RT-PCR to reduce mouse-to-mouse variation. Primers were used to detect mouse β-casein, mouse keratin 18 (K18), transgenic bacterial rtTA, or human ErbB4 transcripts. Human ErbB4 primers flanked the 48-bp region of $s80^{Cyt1}$ that is absent from $s80^{Cyt2}$ to discriminate between the two isoforms based on amplicon size. Genotypes are indicated at the top of the panels. Samples in the last lane were analyzed without RT (−Rv.Tr.). (F and G) Phospho-Tyr694-STAT5a/STAT5b in 6-week-old virgin MTB/Cyt1 mice treated with DOX for 96 h or left untreated. (H) Top panel: Northern analysis (using a β-casein cDNA probe) of total mammary RNA from mice left untreated or treated with DOX for 96 h. Lower panel: corresponding ethidium-stained RNA gel. Genotypes are indicated at the top of the panels. (I to L) Mice (12 weeks of age) were left untreated or treated with DOX from 0.5 dpc to L10. The arrow in panel L indicates focal hyperplasia. Representative hematoxylin- and eosin-stained sections of mammary glands are shown.

not decrease growth of the LA epithelium (Fig. 7D to F and G). However, numerous $PCNA^+$ LA cells were identified at L10 in mammary glands from DOX-treated MTB/Cyt2 mice. Therefore, proliferative stimulation by $s80^{Cyt2}$ is not limited to the ductal epithelium. Whereas $s80^{Cyt2}$ expression during pregnancy did not further increase proliferation in the already highly proliferative LA epithelium, $s80^{Cyt2}$ expression continued to drive cellular proliferation in cells that would normally exit the cell cycle.

To test the cell type specificity of $s80^{Cyt1}$-mediated growth inhibition, we examined the mammary epithelium at early pregnancy (7.5 dpc) in MTB/Cyt1 mice. DOX treatment commenced at 3 weeks of age, pregnancies were established at 8 weeks of age (mid-to-late puberty), and mammary glands were harvested at 9 weeks of age (late puberty simultaneous with early pregnancy). We compared MTB/Cyt1 mammary glands from pregnant and pubertal mice (Fig. 7H) to MTB/Cyt1 mammary glands from virgin and pubertal mice (Fig. 7I) in order to specifically examine ductal growth inhibition in the presence or absence of early LA development. To rule out the effects of DOX treatment on ductal versus LA growth, pubertal and virgin TetOp-Cyt1 siblings were also examined (Fig. 7J).

Decreased lengthening of the ductal epithelium was again seen in DOX-treated MTB/s80 mice (see Fig. 4), regardless of whether the mice were pregnant or virgin (Fig. 7H to J). TEBs characteristic of the growing, pubertal ductal epithelium were evident in mammary glands expressing GFP-$s80^{Cyt1}$ but had already regressed in control, DOX-treated TetOp-Cyt1 mice. These data confirm that lengthening of the ductal epithelium was impaired by expression of $s80^{Cyt1}$ in both virgin and pregnant mice. However, even though ductal length was decreased in pregnant DOX-treated MTB/Cyt1 mice, developing LA structures (typical of the mammary gland during pregnancy) were readily apparent. Therefore, expression of GFP-$s80^{Cyt1}$

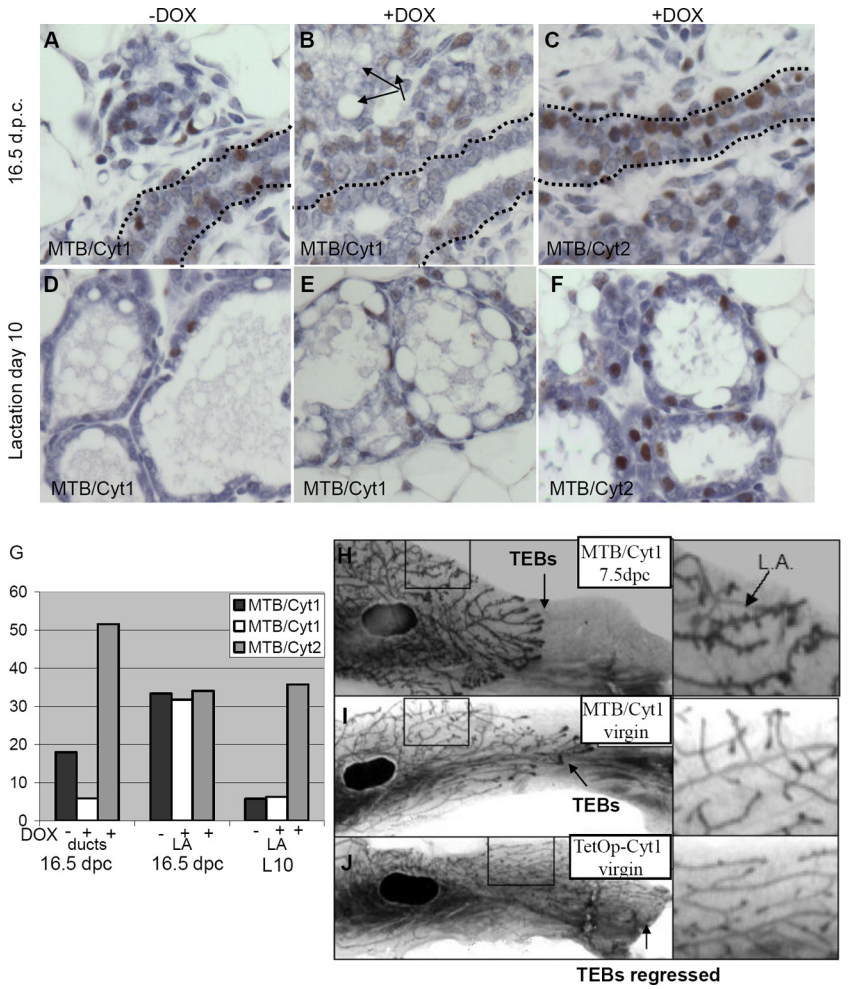

FIG. 7. Growth inhibition in the ductal epithelium but not the LA epithelium in response to expression of s80^{Cyt1}. (A to F) PCNA IHC analysis of mammary sections treated with DOX until 16.5 dpc or left untreated was withheld until mice were 12 weeks of age. DOX treatment began at 0.5 dpc and was maintained through 16.5 dpc (A to C) or through L10 (D to F). Ductal epithelia are indicated by outlining in panels A to C. Arrows in panel B indicate lipid droplet formation. (G) Quantitation of the percentages of epithelial cells that were PCNA$^+$ in ducts and LA at 16.5 dpc and at L10. (H to J) Mice were treated with DOX beginning at 3 weeks of age. Pregnancy (H) was timed in specified animals beginning at 8 weeks. Mammary glands from age-matched DOX-treated virgin or pregnant (7.5 dpc) mice were analyzed in parallel. Images represent whole-mount hematoxylin-stained mammary glands, showing pregnancy-induced LA development in the same gland in which s80^{Cyt1} has retarded ductal elongation. Boxed areas are enlarged at right to show detail. Arrows indicate location of TEBs in panels H and I and lack of TEBs in panel J.

differentially affects these two cell populations of the mammary epithelium.

Increased β-catenin signaling in mammary glands expressing s80^{Cyt2}. To determine the mechanisms by which GFP-s80^{Cyt2} may increase growth of MECs, we examined members of several signaling pathways known to affect growth of the mammary epithelium. Levels of p53 and NF-κB phospho-p65 (as determined by IHC) and levels of phospho-ErbB1 and phospho-ErbB2 (as determined by IP of each from mammary extracts, followed by phosphotyrosine immunoblot analysis) were unaltered in mammary glands expressing GFP-s80^{Cyt1} or GFP-s80^{Cyt2} compared to controls (data not shown). However, IHC revealed elevated levels of c-myc (Fig. 8A to D) and cyclin D1 (Fig. 8E to H) in mammary glands expressing GFP-s80^{Cyt2} but not in mammary glands expressing GFP-s80^{Cyt1}. Because the genes encoding both c-myc and cyclin D1 are transcriptional targets of β-catenin, we examined expression and subcellular localization of β-catenin by IHC (Fig. 8I to L). Moderate levels of β-catenin were observed to have localized to the plasma membrane in the MECs of vehicle-treated controls (Fig. 8I to J) and DOX-treated MTB/Cyt1 mice (Fig. 8K). In contrast, mammary glands from DOX-treated MTB/Cyt2 mice displayed an increased intensity of β-catenin staining localized to nuclei and cytoplasm (Fig. 8L), indicating β-catenin stabilization in mammary glands expressing GFP-s80^{Cyt2}.

IHC detection of E-cadherin demonstrated abundant cell surface localization of E-cadherin in the ductal epithelium of mammary glands harvested from vehicle-treated mice or from DOX-treated MTB/Cyt1 mice (Fig. 8M to P). However, E-cadherin expression was reduced in ductal epithelial cells expressing s80^{Cyt2}.

Wnts are secreted ligands that bind to cell surface receptors, resulting in stabilization and nuclear localization of β-catenin. Multiple members of the Wnt family (Wnt1, Wnt2, Wnt10a,

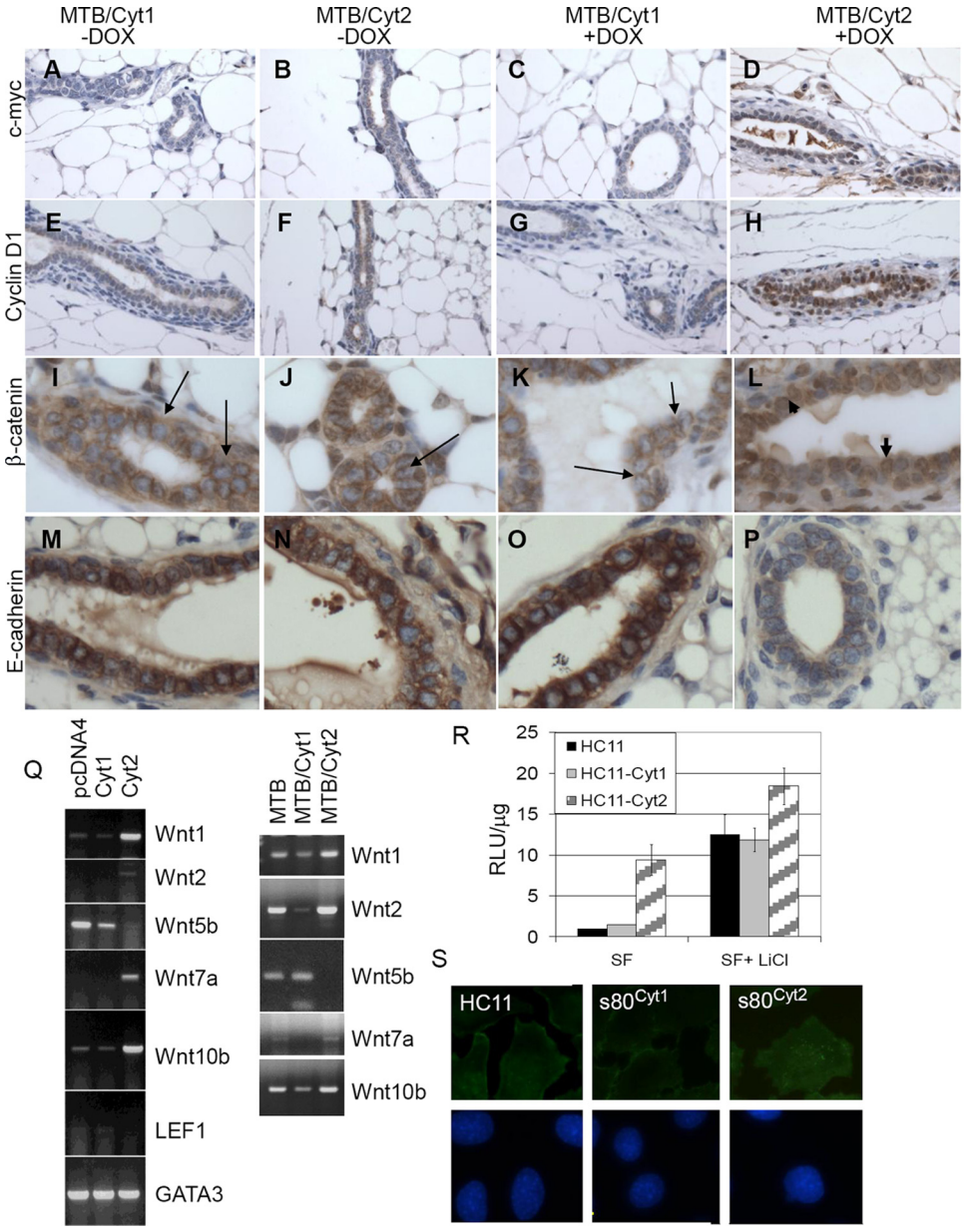

FIG. 8. Stabilization and nuclear localization of β-catenin in cells expressing $s80^{Cyt2}$ but not in cells expressing $s80^{Cyt1}$. (A to P) IHC detection of c-myc (A to D), cyclin D1 (E to H), β-catenin (I to L), and E-cadherin (M to P) in mammary glands from virgin 6-month-old female mice left untreated or treated with DOX from 3 weeks of age. Arrows indicate nuclei lacking β-catenin localization. Arrowheads indicate nuclear β-catenin. (Q) RT-PCR analysis of total cellular RNA harvested from HC11-pcDNA4, HC11-$s80^{Cyt1}$, and HC11-$s80^{Cyt2}$ cells growing in 10% serum (left panel) or from virgin female MTB, MTB/Cyt1, and MTB/Cyt2 mice treated with DOX for 96 h (right panel). Primers specific for the transcripts indicated at the right of each panel were used. (R) Cells were transfected with a TCF/LEF-dependent promoter-firefly luciferase reporter and a constitutive Renilla luciferase reporter and cultured in serum-free (SF) media or in serum-free media with 10 mM LiCl. At 48 h after transfection, whole-cell extracts were analyzed; data represent relative light units (RLU). Values shown are normalized to numbers of relative light units per microgram observed in untreated HC11-pcDNA4 cells. Data represent average values (± standard deviations) determined in three experiments, each analyzed in triplicate. (S) Immunofluorescence detection of β-catenin in cells growing in media with 10% serum.

and Wnt7) are associated with tumorigenesis in the mammary epithelium, whereas others (Wnt5b) are associated with differentiation of the LA epithelium in response to the presence of progesterone (51, 31). Expression of each of these ligands in HC11 cells expressing GFP-$s80^{Cyt1}$ and GFP-$s80^{Cyt2}$ was examined by RT-PCR (Fig. 8Q). Increased expression of the proliferative Wnts (Wnt1, Wnt2, Wnt7, and Wnt10b) was observed in RNA from HC11-$s80^{Cyt2}$ cells but was detected only at very low levels in HC11-pcDNA4 and HC11-$s80^{Cyt1}$ cells. In contrast, Wnt5b (associated with LA differentiation) was detected in HC11-$s80^{Cyt1}$ cells but not in HC11-$s80^{Cyt2}$ cells. Using RNA harvested from mammary glands of virgin, DOX-treated MTB, MTB/Cyt1, and MTB/Cyt2 mice, an increase in the levels of transcripts encoding Wnt1, Wnt2, and Wnt10b

was detected in mammary glands expressing $s80^{Cyt2}$ compared to control mammary glands (Fig. 8Q). The level of each of these transcripts encoding the proliferative Wnts was decreased in mammary glands from MTB/Cyt1 mice. Wnt5b was not detected in MTB/Cyt2 mammary glands but was readily detected in mammary glands expressing $s80^{Cyt1}$. Taken together, these data suggest that proliferative Wnts are expressed at higher levels in mammary epithelial cells expressing $s80^{Cyt2}$ but not in those cells expressing $s80^{Cyt1}$.

To further assess the relative levels of β-catenin-dependent transcriptional activity in HC11 cells expressing GFP-$s80^{Cyt1}$ and GFP-$s80^{Cyt2}$, a β-catenin reporter construct harboring a promoter activated by transcription factors of the β-catenin-dependent TCF/LEF family was used. Increased levels of β-catenin-dependent luciferase were detected in HC11-$s80^{Cyt2}$ cells compared to HC11-$s80^{Cyt1}$ cells (Fig. 8R). As a positive control for each sample, addition of LiCl was used to inhibit GSK-3β, therefore stabilizing the β-catenin content. Addition of LiCl increased luciferase activity over what was seen under basal conditions in all samples, but the activity was again greatest in HC11-$s80^{Cyt2}$ cells. Membrane localization of β-catenin in HC11 cells and in HC11-$s80^{Cyt1}$ cells was observed by immunocytofluorescence determinations (Fig. 8S). However, β-catenin did not display membrane localization in HC11-$s80^{Cyt2}$ cells but rather was located diffusely in the cytoplasm and nucleus. These data, taken together, suggest that increased Wnt signaling results in cytoplasmic accumulation and nuclear localization of β-catenin, which may increase growth of cells in response to GFP-$s80^{Cyt2}$.

DISCUSSION

Despite extensive studies into the role and the prognostic value of ErbB receptors in breast cancer, the significance of ErbB4 has remained unresolved (9), partly due to its unique biology within the ErbB family as a cytoplasmic and nuclear signaling molecule and partly due to the splice variations of ErbB4 which increase the complexity of ErbB4 signaling outcomes (15, 16, 41, 42, 54). We have developed cell culture and mouse models to compare directly the effects of the two cytoplasmic ErbB4 isoforms on development and homeostasis of MECs. Alternative splicing generates these two naturally occurring isoforms, both of which have been previously detected in normal human mammary tissue, clinical breast cancer specimens, and breast cancer cell lines. Although they differ from each other by only 16 amino acids, expression of one isoform ($s80^{Cyt1}$) results in a phenotype that is diametrically opposed to the phenotype produced by the other ($s80^{Cyt2}$).

Expression of $s80^{Cyt1}$ results in profound growth inhibition and precocious differentiation of the ductal epithelium (Fig. 4 and 7). The ability of $s80^{Cyt1}$ to inhibit growth and enhance differentiation of MECs may explain why ErbB4 expression correlates with a more favorable prognosis in many breast cancer studies. Data presented here demonstrate that one aspect of ErbB4 signaling, the production of $s80^{Cyt1}$, is sufficient to initiate some of the molecular aspects of lactogenic differentiation in the absence of the hormonal signals of pregnancy. Additionally, this is the first demonstration that $s80^{Cyt1}$ is far more potent in inducing differentiation than $s80^{Cyt2}$. In the models tested, in fact, $s80^{Cyt2}$ had little or no effect on differentiated gene expression. This was seen in vivo, as well as in 3D HC11 cultures, in which expression of $s80^{Cyt1}$ resulted in the formation of lumen-containing acinar structures, a process that has previously been shown to require JAK2 and STAT5a activity (52). In contrast, expression of $s80^{Cyt2}$ in HC11 cells resulted in the organization of solid epithelial spheres harboring an increased number of cells. The reasons for differential structural organization due to $s80^{Cyt1}$ versus $s80^{Cyt2}$ expression are not obvious at this point, especially in light of reports that STAT5a phosphorylation (but not transcriptional activation) is induced by expression of either $s80^{Cyt1}$ or $s80^{Cyt2}$ in serum-starved cells (25, 42). Increased levels of E-cadherin in $s80^{Cyt1}$-expressing cells (Fig. 6) or in those expressing ErbB4-JMa-Cyt1 (33) may promote epithelial polarization and adherens junction formation, both of which are required for lumen formation. Interestingly, STAT5a activation is known to stabilize E-cadherin accumulation at the cell surface, promote homotypic cell-cell adhesion, and stabilize β-catenin–E-cadherin interactions in breast epithelial cells in culture (40). Given that $s80^{Cyt1}$ promotes STAT5a activation to a greater degree than does $s80^{Cyt2}$, it is possible that the $s80^{Cyt1}$-STAT5a complex functions in epithelial cells to enhance E-cadherin accumulation at the cell surface. Another hypothesis is that a certain level of growth inhibition in response to $s80^{Cyt1}$ expression primes the mammary epithelium for lumen formation or lactational differentiation in a STAT5a-dependent manner. Conversely, the proliferative capacity of MECs expressing $s80^{Cyt2}$ may prevent STAT5a-mediated differentiation in the absence of pregnancy-induced hormones.

Intriguingly, growth inhibition via expression of $s80^{Cyt1}$ was limited to the ductal epithelium of the mammary gland, as expression of $s80^{Cyt1}$ at an equivalent level did not decrease growth of LA structures during pregnancy. This observation highlights a cellular specificity of $s80^{Cyt1}$-mediated growth inhibition within the mammary epithelium and underscores the idea that, despite the common origin of these two epithelial populations, the biology of each is unique. This also demonstrates that the level of DOX-induced $s80^{HER4}$ expression has specific rather than general effects; that is, it does not result in growth inhibition in all cell populations.

In direct contrast to $s80^{Cyt1}$-mediated differentiation, $s80^{Cyt2}$ expression results in epithelial hyperplasia, with increased expression and nuclear localization of β-catenin, a protein involved in both cellular adhesion (when associated with the E-cadherin–actin complex found at adherens junctions) and tumor progression (reviewed in reference 31). Cytosolic β-catenin, resulting from the disruption of β-catenin–E-cadherin interactions, is rapidly degraded in quiescent cells. Growth factor signaling can stabilize free β-catenin, which translocates to the nucleus, binds TCF/LEF transcription factors, and induces the expression of target genes, including c-*myc* and *cyclin D1*. As is consistent with this model of β-catenin signaling, mammary glands expressing $s80^{Cyt2}$ also showed increased levels of cyclin D1 and c-myc. Interestingly, studies have shown that the ErbB receptors EGFR/ErbB1 and ErbB2 can induce tyrosine phosphorylation of β-catenin, destabilizing the β-catenin–E-cadherin interaction while increasing invasion and metastasis in breast cancer cell lines (11, 30, 34, 36). Although these studies focused primarily on ErbB1 and -2,

they indicate that certain members of the ErbB receptor kinase family cooperate with β-catenin in tumorigenesis.

Interestingly, ErbB4-JMa-Cyt2 was overexpressed in a subset of human breast cancer specimens (22), supporting the notion that $s80^{Cyt2}$ may confer a growth advantage to human tumor cells. To determine the potential prognostic information and therapeutic consequences of the presence of Cyt2 and Cyt1 in cases of human breast cancer, it will be important to understand the mechanism by which each ErbB4 isoform acts. ErbB4 isoform Cyt2 lacks the 16-amino-acid insert and has the proliferative signaling capacity described above. The 16-amino-acid insert provides Cyt1 with at least two signaling motifs: (i) phosphorylation at Y1056 yields a PI3 kinase interaction site (5), and (ii) residues 1052 to 1056 (PPPAY) bind WW domain-containing proteins (1, 2). Several WW domain-containing proteins, including the transcription factor YAP and Wwox, a known tumor suppressor protein that has been found to be deleted in many cases of breast cancer, have been shown to interact with $s80^{HER4}$. Wwox expression in breast cancer has recently been correlated with a more favorable prognosis and with expression of membrane-bound ErbB4 (1). The stability and perhaps signaling of the isoforms may be altered by Itch and WWP1, another WW domain-containing E3-ubiquitin ligase that displays stronger binding and degradation activity toward $s80^{Cyt1}$ than toward $s80^{Cyt2}$ (7, 29, 41). How these and other interactions lead to the unique Cyt1 actions remains to be determined.

In summary, while the in vitro and in vivo models using $s80^{Cyt1}$ and $s80^{Cyt2}$ show levels of expression that are higher than endogenous levels, the multiple data sets clearly define ErbB4 pathways as either growth inhibitory or growth enhancing, depending upon the isoform and the cell type in which ErbB4 is expressed. Given the complexity of ErbB4 isoform biology, the lack of uniformity in published results regarding ErbB4 action, and the clinical significance of ErbB4, it will be important to develop methods to identify each isoform in clinical specimens and to understand the prognostic value of ErbB4 in the context of isoform specificity.

ACKNOWLEDGMENTS

The research was supported by the Breast Cancer Research Foundation and NIH grant RO1 CA112553 and the UNC Breast Cancer SPORE (grant 1-P50-CA058223-17).

REFERENCES

1. **Aqeilan, R. I., V. Donati, E. Gaudio, M. S. Nicoloso, M. Sundvall, A. Korhonen, J. Lundin, J. Isola, M. Sudol, H. Joensuu, C. M. Croce, and K. Elenius.** 2007. Association of Wwox with ErbB4 in breast cancer. Cancer Res. **67:**9330–9336.
2. **Aqeilan, R. I., V. Donati, A. Palamarchuk, F. Trapasso, M. Kaou, Y. Pekarsky, M. Sudol, and C. M. Croce.** 2005. WW domain-containing proteins, WWOX and YAP, compete for interaction with ErbB-4 and modulate its transcriptional function. Cancer Res. **65:**6764–6772.
3. **Barnes, N. L., S. Khavari, G. P. Boland, A. Cramer, W. F. Knox, and N. J. Bundred.** 2005. Absence of HER4 expression predicts recurrence of ductal carcinoma in situ of the breast. Clin. Cancer Res. **11:**2163–2168.
4. **Chen, Q. Q., X. Y. Chen, Y. Y. Jiang, and J. Liu.** 2005. Identification of novel nuclear localization signal within the ErbB-2 protein. Cell Res. **15:**504–510.
5. **Elenius, K., C. J. Choi, S. Paul, E. Santiestevan, E. Nishi, and M. Klagsbrun.** 1999. Characterization of a naturally occurring ErbB4 isoform that does not bind or activate phosphatidyl inositol 3-kinase. Oncogene **18:**2607–2615.
6. **Elenius, K., G. Corfas, S. Paul, C. J. Choi, C. Rio, G. D. Plowman, and M. Klagsbrun.** 1997. A novel juxtamembrane domain isoform of HER4/ErbB4. Isoform-specific tissue distribution and differential processing in response to phorbol ester. J. Biol. Chem. **272:**26761–26768.
7. **Feng, S. M., R. S. Muraoka-Cook, D. Hunter, M. A. Sandahl, L. S. Caskey, K. Miyazawa, A. Atfi, and H. S. Earp III.** 2009. The E3 ubiquitin ligase WWP1 selectively targets HER4 and its proteolytically derived signaling isoforms for degradation. Mol. Cell. Biol. **29:**892–906.
8. **Feng, S. M., C. I. Sartor, D. Hunter, H. Zhou, X. Yang, L. S. Caskey, R. Dy, R. S. Muraoka-Cook, and H. S. Earp III.** 2007. The HER4 cytoplasmic domain, but not its C terminus, inhibits mammary cell proliferation. Mol. Endocrinol. **21:**1861–1876.
9. **Gullick, W. J.** 2003. c-erbB-4/HER 4, friend or foe? J. Pathol. **200:**279–281.
10. **Gunther, E. J., G. K. Belka, G. B. Wertheim, J. Wang, J. L. Hartman, R. B. Boxer, and L. A. Chodosh.** 2002. A novel doxycycline-inducible system for the transgenic analysis of mammary gland biology. FASEB J. **16:**283–292.
11. **Hazan, R. B., and L. Norton.** 1998. The epidermal growth factor receptor modulates the interaction of E-cadherin with the actin cytoskeleton. J. Biol. Chem. **273:**9078–9084.
12. **Holbro, T., and N. E. Hynes.** 2004. ErbB receptors: directing key signaling networks throughout life. Annu. Rev. Pharmacol. Toxicol. **44:**195–217.
13. **Jones, F. E., J. P. Golding, and M. Gassmann.** 2003. ErbB4 signaling during breast and neural development: novel genetic models reveal unique ErbB4 activities. Cell Cycle **2:**555–559.
14. **Jones, F. E., T. Welte, X. Y. Fu, and D. F. Stern.** 1999. ErbB4 signaling in the mammary gland is required for lobuloalveolar development and Stat5 activation during lactation. J. Cell Biol. **147:**77–88.
15. **Junttila, T. T., M. Sundvall, M. Lundin, J. Lundin, M. Tanner, P. Harkonen, H. Joensuu, J. Isola, and K. Elenius.** 2005. Cleavable ErbB4 isoform in estrogen receptor-regulated growth of breast cancer cells. Cancer Res. **65:**1384–1393.
16. **Kainulainen, V., M. Sundvall, J. A. Määttä, E. Santiestevan, M. Klagsbrun, and K. Elenius.** 2000. A natural ErbB4 isoform that does not activate phosphoinositide 3-kinase mediates proliferation but not survival or chemotaxis. J. Biol. Chem. **275:**8641–8649.
17. **Kim, J., W. J. Jahng, D. Di Vizio, J. S. Lee, R. Jhaveri, M. A. Rubin, A. Shisheva, and M. R. Freeman.** 2007. The phosphoinositide kinase PIKfyve mediates epidermal growth factor receptor trafficking to the nucleus. Cancer Res. **67:**9229–9237.
18. **Lee, H. J., K. M. Jung, Y. Z. Huang, L. B. Bennett, J. S. Lee, L. Mei, and T. W. Kim.** 2002. Presenilin-dependent gamma-secretase-like intramembrane cleavage of ErbB4. J. Biol. Chem. **277:**6318–6323.
19. **Lin, S. Y., K. Makino, W. Xia, A. Matin, Y. Wen, K. Y. Kwong, L. Bourguignon, and M. C. Hung.** 2001. Nuclear localization of EGF receptor and its potential new role as a transcription factor. Nat. Cell Biol. **3:**802–808.
20. **Linggi, B., Q. C. Cheng, A. R. Rao, and G. Carpenter.** 2006. The ErbB-4 s80 intracellular domain is a constitutively active tyrosine kinase. Oncogene **25:**160–163.
21. **Long, W., K. U. Wagner, K. C. Lloyd, N. Binart, J. M. Shillingford, L. Hennighausen, and F. E. Jones.** 2003. Impaired differentiation and lactational failure of Erbb4-deficient mammary glands identify ERBB4 as an obligate mediator of STAT5. Development **130:**5257–5268.
22. **Määttä, J. A., M. Sundvall, T. T. Junttila, L. Peri, V. J. Laine, J. Isola, M. Egeblad, and K. Elenius.** 2006. Proteolytic cleavage and phosphorylation of a tumor-associated ErbB4 isoform promote ligand-independent survival and cancer cell growth. Mol. Biol. Cell **17:**67–79.
23. **Muraoka, R. S., A. E. Lenferink, J. Simpson, D. M. Brantley, L. R. Roebuck, F. M. Yakes, and C. L. Arteaga.** 2001. Cyclin-dependent kinase inhibitor p27(Kip1) is required for mouse mammary gland morphogenesis and function. J. Cell Biol. **153:**917–932.
24. **Muraoka-Cook, R. S., L. S. Caskey, M. A. Sandahl, D. M. Hunter, C. Husted, K. E. Strunk, C. I. Sartor, W. A. Rearick, Jr., W. McCall, M. K. Sgagias, K. H. Cowan, and H. S. Earp III.** 2006. Heregulin-dependent delay in mitotic progression requires HER4 and BRCA1. Mol. Cell. Biol. **26:**6412–6424.
25. **Muraoka-Cook, R. S., M. A. Sandahl, C. Husted, D. M. Hunter, L. C. Miraglia, S.-M. Feng, K. Elenius, and H. S. Earp III.** 2006. The intracellular domain of ErbB4 induces differentiation of mammary epithelial cells. Mol. Biol. Cell **17:**4118–4129.
26. **Naresh, A., W. Long, G. A. Vidal, W. C. Wimley, L. Marrero, C. I. Sartor, S. Tovey, T. G. Cooke, J. M. Bartlett, and F. E. Jones.** 2006. The ERBB4/HER4 intracellular domain 4ICD is a BH3-only protein promoting apoptosis of breast cancer cells. Cancer Res. **66:**6412–6420.
27. **Ni, C. Y., M. P. Murphy, T. E. Golde, and G. Carpenter.** 2001. γ-Secretase cleavage and nuclear localization of ErbB-4 receptor tyrosine kinase. Science **294:**2179–2181.
28. **Offterdinger, M., C. Schofer, K. Weipoltshammer, and T. W. Grunt.** 2002. c-erbB-3: a nuclear protein in mammary epithelial cells. J. Cell Biol. **157:**929–939.
29. **Omerovic, J., L. Santangelo, E. M. Puggioni, J. Marrocco, C. Dall'Armi, C. Palumbo, F. Belleudi, L. Di Marcotullio, L. Frati, M. R. Torrisi, G. Cesareni, A. Gulino, and M. Alimandi.** 2007. The E3 ligase Aip4/Itch ubiquitinates and targets ErbB-4 for degradation. FASEB J. **21:**2849–2862.
30. **Piedra, J., D. Martinez, J. Castano, S. Miravet, M. Dunach, and A. G. de Herreros.** 2001. Regulation of β-catenin structure and activity by tyrosine phosphorylation. J. Biol. Chem. **276:**20436–20443.
31. **Polakis, P.** 2000. Wnt signaling and cancer. Genes Dev. **14:**1837–1851.
32. **Rio, C., J. D. Buxbaum, J. J. Peschon, and G. Corfas.** 2000. Tumor necrosis

factor-alpha-converting enzyme is required for cleavage of erbB4/HER4. J. Biol. Chem. **275:**10379–10387.
33. **Sartor, C. I., H. Zhou, E. Kozlowska, K. Guttridge, E. Kawata, L. Caskey, J. Harrelson, N. Hynes, S. Ethier, B. Calvo, and H. S. Earp III.** 2001. HER4 mediates ligand-dependent antiproliferative and differentiation responses in human breast cancer cells. Mol. Cell. Biol. **21:**4265–4275.
34. **Schroeder, J. A., M. C. Adriance, E. J. McConnell, M. C. Thompson, B. Pockaj, and S. J. Gendler.** 2002. ErbB-β-catenin complexes are associated with human infiltrating ductal breast and murine mammary tumor virus (MMTV)-Wnt-1 and MMTV-c-Neu transgenic carcinomas. J. Biol. Chem. **277:**22692–22698.
35. **Schroeder, J. A., and D. C. Lee.** 1998. Dynamic expression and activation of ERBB receptors in the developing mouse mammary gland. Cell Growth Differ. **9:**451–464.
36. **Shibata, T., A. Ochiai, Y. Kanai, S. Akimoto, M. Gotoh, N. Yasui, R. Machinami, and S. Hirohashi.** 1996. Dominant negative inhibition of the association between beta-catenin and c-erbB-2 by N-terminally deleted beta-catenin suppresses the invasion and metastasis of cancer cells. Oncogene **13:**883–889.
37. **Srinivasan, R., C. E. Gillett, D. M. Barnes, and W. J. Gullick.** 2000. Nuclear expression of the c-erbB-4/HER-4 growth factor receptor in invasive breast cancers. Cancer Res. **60:**1483–1487.
38. **Stern, D. F.** 2003. ErbBs in mammary development. Exp. Cell Res. **284:** 89–98.
39. **Strunk, K. E., C. Husted, L. C. Miraglia, M. Sandahl, W. A. Rearick, D. M. Hunter, H. S. Earp III, and R. S. Muraoka-Cook.** 2007. HER4 D-box sequences regulate mitotic progression and degradation of the nuclear HER4 cleavage product $s80^{HER4}$. Cancer Res. **67:**6582–6590.
40. **Sultan, A. S., J. Xie, M. J. LeBaron, E. L. Ealley, M. T. Nevalainen, and H. Rui.** 2005. Stat5 promotes homotypic adhesion and inhibits invasive characteristics of human breast cancer cells. Oncogene **24:**746–760.
41. **Sundvall, M., A. Korhonen, I. Paatero, E. Gaudio, G. Melino, C. M. Croce, R. I. Aqeilan, and K. Elenius.** 2008. Isoform-specific monoubiquitination, endocytosis, and degradation of alternatively spliced ErbB4 isoforms. Proc. Natl. Acad. Sci. USA **105:**4162–4167.
42. **Sundvall, M., L. Peri, J. A. Määttä, D. Tvorogov, I. Paatero, M. Savisalo, O. Silvennoinen, Y. Yarden, and K. Elenius.** 2007. Differential nuclear localization and kinase activity of alternative ErbB4 intracellular domains. Oncogene **26:**6905–6914.
43. **Suo, Z., B. Risberg, M. G. Kalsson, et al.** 2002. EGFR family expression in breast carcinomas. c-erbB-2 and c-erbB-4 receptors have different effects on survival. J. Pathol. **196:**17–25.
44. **Tidcombe, H., A. Jackson-Fisher, K. Mathers, D. F. Stern, M. Gassmann, and J. P. Golding.** 2003. Neural and mammary gland defects in ErbB4 knockout mice genetically rescued from embryonic lethality. Proc. Natl. Acad. Sci. USA **100:**8281–8286.
45. **Tovey, S. M., C. J. Witton, J. M. Bartlett, P. D. Stanton, J. R. Reeves, and T. G. Cooke.** 2004. Outcome and human epidermal growth factor receptor (HER) 1–4 status in invasive breast carcinomas with proliferation indices evaluated by bromodeoxyuridine labelling. Breast Cancer Res. **6:**R246–R251.
46. **Vidal, G. A., A. Narres, L. Marrero, and F. E. Jones.** 2005. Presenilin-dependent gamma-secretase processing regulates multiple ERBB4/HER4 activities. J. Biol. Chem. **280:**19777–19783.
47. **Wang, S. C., H. C. Lien, W. Xia, I. F. Chen, H. W. Lo, Z. Wang, M. Ali-Seyed, D. F. Lee, G. Bartholomeusz, F. Ou-Yang, D. K. Giri, and M. C. Hung.** 2004. Binding at and transactivation of the COX-2 promoter by nuclear tyrosine kinase receptor ErbB-2. Cancer Cell **6:**251–261.
48. **Williams, C. C., J. G. Allison, G. A. Vidal, M. E. Burow, B. S. Beckman, L. Marrero, and F. E. Jones.** 2004. The ERBB4/HER4 receptor tyrosine kinase regulates gene expression by functioning as a STAT5A nuclear chaperone. J. Cell Biol. **167:**469–478.
49. **Wiseman, S. M., N. Makretsov, T. O. Nielsen, B. Gilks, E. Yorida, M. Cheang, D. Turbin, K. Gelmon, and D. G. Huntsman.** 2005. Coexpression of the type 1 growth factor receptor family members HER-1, HER-2, and HER-3 has a synergistic negative prognostic effect on breast carcinoma survival. Cancer **103:**1770–1777.
50. **Witton, C. J., J. R. Reeves, J. J. Going, T. G. Cooke, and J. M. Bartlett.** 2003. Expression of the HER1-4 family of receptor tyrosine kinases in breast cancer. J. Pathol. **200:**290–297.
51. **Wong, G. T., B. J. Gavin, and A. P. McMahon.** 1994. Differential transformation of mammary epithelial cells by Wnt genes. Mol. Cell. Biol. **14:**6278–6286.
52. **Xie, J., M. J. LeBaron, M. T. Nevalainen, and H. Rui.** 2002. Role of tyrosine kinase Jak2 in prolactin-induced differentiation and growth of mammary epithelial cells. J. Biol. Chem. **277:**14020–14030.
53. **Yu, W. H., J. F. Woessner, Jr., J. D. McNeish, and I. Stamenkovic.** 2002. CD44 anchors the assembly of matrilysin/MMP-7 with heparin-binding epidermal growth factor precursor and ErbB4 and regulates female reproductive organ remodeling. Genes Dev. **16:**307–323.
54. **Zeng, F., M. Z. Zhang, A. B. Singh, R. Zent, and R. C. Harris.** 2007. ErbB4 isoforms selectively regulate growth factor induced Madin-Darby canine kidney cell tubulogenesis. Mol. Biol. Cell **18:**4446–4456.
55. **Zhu, Y., L. L. Sullivan, S. S. Nair, C. C. Williams, A. K. Pandey, L. Marrero, R. K. Vadlamudi, and F. E. Jones.** 2006. Coregulation of estrogen receptor by ERBB4/HER4 establishes a growth-promoting autocrine signal in breast tumor cells. Cancer Res. **66:**7991–7998.